Z. Phys. C – Particles and Fields 46, 349–359 (1990)

Zeitschrift für Physik C Particles and Fields

A measurement of the weak axial couplings of the *b*- and *c*-quark

JADE Collaboration

E. Elsen[3], J. Allison[5], K. Ambrus[3,a], R.J. Barlow[5], W. Bartel[1], S. Bethke[3,b], C.K. Bowdery[4], S.L. Cartwright[7,c], J. Chrin[5], D. Clarke[7], A. Dieckmann[3], I.P. Duerdoth[5], G. Eckerlin[3], R. Felst[1], A.J. Finch[4], F. Foster[4], T. Greenshaw[2], J. Hagemann[2], D. Haidt[1], J. Heintze[3], G. Heinzelmann[2], K.H. Hellenbrand[3,d], P. Hill[6,e], G. Hughes[4], H. Kado[1,f], T. Kawamoto[8], C. Kleinwort[2,b], G. Knies[1], T. Kobayashi[8], S. Komamiya[3,g], H. Krehbiel[1], J. v. Krogh[3], M. Kuhlen[2,h], F.K. Loebinger[5], A.A. Macbeth[5], N. Magnussen[1,i], R. Marshall[7], R. Meinke[1], R.P. Middleton[7], H. Minowa[8], P.G. Murphy[5], B. Naroska[1], J.M. Nye[4], J. Olsson[1], F. Ould-Saada[2], R. Ramcke[1], H. Rieseberg[3], D. Schmidt[1,i], H. von der Schmitt[3], L. Smolik[3], U. Schneekloth[2,j], J.A.J. Skard[6,k], J. Spitzer[3], P. Steffen[1], K. Stephens[5], A. Wagner[3], I.W. Walker[4], G. Weber[2], M. Zimmer[3], G.T. Zorn[6]

[1] Deutsches Elektronen-Synchrotron DESY, Hamburg, Federal Republic of Germany
[2] II. Institut für Experimentalphysik der Universität Hamburg, Hamburg, Federal Republic of Germany
[3] Physikalisches Institut der Universität Heidelberg, Heidelberg, Federal Republic of Germany
[4] University of Lancaster, Lancaster, England
[5] University of Manchester, Manchester, England
[6] University of Maryland, College Park, MD, USA
[7] Rutherford Appleton Laboratory, Chilton, Didcot, England
[8] International Center for Elementary Particle Physics, University of Tokyo, Tokyo, Japan

Received 16 October 1989

Abstract. The forward-backward charge asymmetries of the *b* and *c* quarks are measured with the JADE detector at PETRA at $\sqrt{s}=35$ GeV and 44 GeV using both electrons and muons to tag the heavy quarks. At $\sqrt{s}=35$ GeV, a simultaneous fit for the two asymmetries yields the result $A_b=-9.3\pm5.2\%$ (stat.) and $A_c=-9.6\pm4.0\%$ (stat.). A fit for the *b*-asymmetry alone gives $A_b=-11.6\pm4.8\%$ (stat.). The systematic errors are comparable with the statistical uncertainties. Combining the measurements at both energies and alternately constraining the weak coupling of the *c* and *b* quark to their Standard Model values ($a_c=1$, $a_b=-1$) increases the precision of the measurement of coupling constant of the other quark. Using this procedure $a_b=-0.72\pm0.34$ and $a_c=0.79\pm0.40$, where the numbers are corrected for $B\bar{B}$-mixing and the errors include both statistical and systematic contributions. The mixing parameter for continuum $b\bar{b}$-production is determined to be $\chi=0.24\pm0.12$ if both heavy quark coupling constants are constrained to their values in the Standard Model.

[a] Now at MBB, München, FRG
[b] Now at CERN, Geneva, Switzerland
[c] Now at University of Sheffield, Sheffield, UK
[d] Now at Universität des Saarlandes, Saarbrücken, FRG
[e] Now at DESY, Hamburg, FRG
[f] Now at Bayer AG, Brunsbüttel, FRG
[g] Now at SLAC, California, USA
[h] Now at CALTECH, California, USA
[i] Universität-Gesamthochschule Wuppertal, Wuppertal, FRG
[j] Now at MIT, Cambridge, Mass., USA
[k] Now at ST Systems Corporation, Lanham, Md, USA

1 Introduction

Electroweak interference effects in e^+e^--collisions have been well established for the leptons τ, μ and less accurate for *e*. In the quark sector similar progress has been hampered by the difficulty of isolating a particular flavour. For light quarks the experimental knowledge is rather scarce and mainly restricted to the observation of an average effect [1, 2]. The electroweak charges of the charmed quark have been rather well determined by several experiments [3]. For the *b* quark the pioneering work of [4] led to a statistically significant measurement [5].

This analysis returns to the determination of the electroweak couplings of the *b* and *c* quark for several reasons. The accumulated data samples of the PETRA and PEP experiments allow a second generation of asymmetry measurements with improved statistical accuracy and the first new results have been presented [6, 7]. At the same time the methods of analysis and the understanding of detector and event properties have been con-

siderably refined so that the systematic contributions are under better control. Furthermore, the discovery of non-zero $B\bar{B}$ mixing [8, 9] has changed the interpretation of earlier results for the b quark and necessitates a new investigation for the c sector in cases where explicit constraints for the b quark were used in the analysis.

The analysis presented here makes use of the entire multihadronic data sample of the JADE experiment with $\sqrt{s} \geq 30$ GeV with a detected electron or muon and encompasses the events used in the earlier measurement of the b asymmetry [5]. The leptons serve both as a tag of the heavy quarks b and c and as an indicator of the charge of the primary parton. Additional variables are used to enhance the separation of flavours.

2 Event selection and lepton identification

2.1 Apparatus and event selection

Three major components of the JADE detector [10] are of special interest for this analysis. Charged particles are identified in the cylindrical jet chamber which is operated in a magnetic field of 0.48 T. It provides momentum and charge determination and particle identification by dE/dx measurement at up to 48 points along the track of a particle. The electromagnetic shower detector consists of an array of lead glass blocks surrounding the jet chamber outside the magnet coil. It is used for the reconstruction of photons and aids in the identification of electrons. The muon filter [11] consists of four successive layers of absorber material interleaved with layers of drift chambers.

Multihadronic events with $\sqrt{s} \geq 30$ GeV are selected using standard JADE criteria which are described in [12]. The sample is dominated by the events at $\sqrt{s} = 35$ GeV (Table 1).

The lepton search described in the following is restricted to events with more than two charged particles per hemisphere in order to reduce the contribution of radiative events of the type $q\bar{q}\gamma$. For both types of leptons an upper momentum cut $p < 10$ GeV/c reduces the background from imperfectly measured particles. The number of leptons found in the data samples after these additional requirements are summarized in Table 1.

For the data period of 1986 ($\sqrt{s} = 35$ GeV) the readout electronics of the jet chamber were replaced by Flash-ADCs [13]. As a result the space resolution in the drift direction was improved for all charged tracks including those in a jet. These differences are allowed for by analysing the various data samples of Table 1 separately and by combining the individual measurements to obtain the final result. We refer to the periods as "1986", "1985" and "1982" as a reminder of the year when most of the data were collected.

Table 1. Event sample

$\langle\sqrt{s}\rangle$ [GeV]	Period	Hadronic events	Leptons	
			e	μ
34.9	1982	26058	931	1724
35.0	1986	28868	808	2002
43.7	1985	9113	368	862

2.2 Electron identification

Electrons are identified by their energy loss in the gas of the jet chamber and by the shower energy deposition in the electromagnetic calorimeter. The identification is confined to the barrel part of the shower detector ($|\cos\theta| < 0.76$), where the resolution is best. A particle is accepted as an electron candidate if the following criteria are fulfilled:

- The measured energy loss is compatible with that of an electron

$$-\sigma < (dE/dx)_{\text{meas}} - (dE/dx)_{\text{electron}} < 2\sigma.$$

- The shape of the electromagnetic shower is consistent with that of an electron.
- There is no other charged particle that can be combined with the candidate particle to form a photon conversion pair.
- The deposited energy E in the lead glass agrees with the momentum measurement p in the jet chamber, i.e. $0.8 < E/p$.

Details of the identification can be found in [14]. The minimum momentum required for electrons is 1.5 GeV/c. This cut is sufficiently high to reduce the large contribution of electrons from conversions and to eliminate the contribution of protons, which yield dE/dx-measurements comparable to those of electrons at momenta around 1 GeV/c. After these cuts the background from hadrons in the sample of electron candidates is estimated to be $\sim 10\%$.

2.3 Muon identification

Muons are identified as penetrating particles in the μ-detector [15]. At least 4.8 absorption lengths have to be traversed by the candidate track. The hits found in the muon detector have to be compatible with the extrapolation of the track from the inner detector taking multiple scattering into account. Muon candidates are required to have at least 1.8 GeV/c momentum to reduce the background from π and K decay.

3 Flavour separation

In the analysis the ideas presented in [4] are refined in several respects and extended to cover the c asymmetry. A Maximum Likelihood analysis is used in the fits so that the full information contained in the events is exploited and the experimental uncertainties intro-

duced by selecting event subsamples are minimized. Quark flavours are separated on a statistical basis using the following three variables:

$p_\perp$: the lepton transverse momentum with respect to the event axis $\mathbf{n}_1$,

$m_\perp$: the "transverse mass",

$$m_\perp = \frac{\sqrt{s}}{E_{\text{vis}}}\left[\left(\sum_{i=\text{lepton}} \sqrt{m_i^2+(\mathbf{p}_i\mathbf{n}_3)^2}\right)^2 - \left(\sum_{i=\text{lepton}} \mathbf{p}_i\mathbf{n}_3\right)^2\right]^{\frac{1}{2}}$$

where $\mathbf{n}_3$ defines the direction perpendicular to the event plane and

$|\cos\theta|$: θ = polar angle of the oriented event axis.

For convenience, the three variables may be considered the components of a vector $\mathbf{m}=(p_\perp, m_\perp, |\cos\theta|)$. The reference directions $\mathbf{n}_i$ are calculated using "linear" event shape measures: $\mathbf{n}_1$ = thrust axis, $\mathbf{n}_2$ = thrust axis of the momentum components after projection onto a plane perpendicular to $\mathbf{n}_1$ and $\mathbf{n}_3=\mathbf{n}_1\times\mathbf{n}_2$. This is the most appropriate choice for the description of jets containing decaying particles and yields an optimum reconstruction of the primary heavy quark direction. The lepton is explicitly excluded from the calculation of $m_\perp$ and also from E_{vis} to reduce experimental correlations with the variable $p_\perp$. E_{vis} is calculated from the energies of the charged and neutral particles. As discussed below, the variable $|\cos\theta|$ has to be added to the set of discriminating variables for purely experimental reasons.

The first two variables are good indicators of the large decay mass of the B-hadrons: While $p_\perp$ is sensitive to the large Q-value of the semileptonic decay, $m_\perp$ is dominated by the high multiplicity of the hadronic decay of the B. For $m_\perp$ there is a residual dependence on the fragmentation function of the B-hadron, introduced by the extra particles not originating from the decay of a B-hadron. We fix the parameter of the fragmentation function to its measured value [16–18] in the simulation of the events* [19, 20] such that within the error of the measurement the residual effect on $m_\perp$ is negligible.

The components "out" of the event plane were used in forming the expression of $m_\perp$ in order to reduce the effects of gluon bremsstrahlung, which to first order produce planar events. We prefer to use the "leading-log" approximation, including QCD coherence effects, in the Monte Carlo simulation. This is known to give a good description of the event properties and especially of the quantities sensitive to the components normal to the event plane. From a phenomenological point of view $m_\perp$ may thus be calculated reliably even for light quarks. The Monte Carlo program includes the full simulation of the resolutions and imperfections of the experimental apparatus. It is used to extract efficiencies and to determine the composition of the lepton sample in terms of "true" leptons and background particles.

* We use the following options of version 6.3 with coherent shower evolution: α_s-scale $z(1-z)m^2$, $\Lambda_{LLA}=0.4$ GeV, $Q_0=1$ GeV, fragmentation parameters $a=0.5$, $b=0.9$ for light quarks (Lund symm. function), $\varepsilon_c=0.05$, $\varepsilon_b=0.01$ for heavy quarks (Peterson et al.) and for $p_\perp$ parameter $\sigma=\sqrt{2}\cdot 0.30$ GeV/c

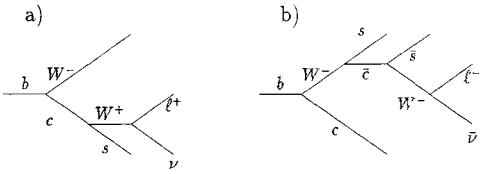

Fig. 1. Leptons from c-mesons in events with primary b-flavour. Only the more frequent diagram a) leads to "natural" charge correlation. Diagram b) shows the same correlation as $b\to l^-$

Table 2. Contribution c_i of the "wrong" charge

Lepton candidate	$b\to l$ c_b	$b\to c\to l$ c_{bc}	$c\to l$ c_c
e	0.5%	13.0%	0.5%
μ	1.0%	24.0%	9.0%

The Monte Carlo simulation is also used to ascertain the association of the lepton charge with the flavour of the generating quark. The "natural" association for a negative lepton l^- is a b or $\bar{c}$. Other associations are also possible, however: Leptons from charm decay in events with primary b flavour may be produced via two virtual Ws, such that the correlation between charge and flavour is the reverse of the natural expectation for the cascade process (Fig. 1). More important from an experimental point of view is the contribution of "fake"-leptons, i.e. misidentified π, K or p, which are not strongly correlated with the charge of the primary quark. Additionally, the charge of the lepton is incorrectly reconstructed with a probability below 1%. Similarly small is the effect of backward decays of the heavy flavour, in which the lepton is emitted into the opposite event hemisphere. This contribution is negligible as a consequence of the hard momentum spectra of the B- and C-hadrons and the minimum momentum requirement on the identified lepton. We define c_i to be the fraction of all contributions leading to the "wrong" charge and extract the values from the Monte Carlo simulation (Table 2). We distinguish the three main categories according to the origin of the lepton candidates. For electrons the charge confusion is mainly restricted to the cascade process $b\to c$. The larger proportion of background particles in the sample of μ-candidates leads to appreciable fractions c_i in charm decay irrespective of the primary flavour of the event.

Both the jet chamber and the electromagnetic calorimeter leave a hole for the beam pipe in the forward and backward directions. Although the pure geometrical loss of acceptance is small (a few per cent of the solid angle) it matters for multiparticle final states. A clear effect can be seen in the reconstruction of the event axis, which relies on all measured particles. This is demonstrated in Fig. 2, where $\langle p_\perp\rangle$ of the leptons is plotted versus $|\cos\theta|$. Even if the lepton is well within the experimental acceptance the event axis is biassed towards the centre of the detector due to particle loss in the forward direction. As a result a decrease in $\langle p_\perp\rangle$ is observed as $|\cos\theta|$ increases from 0 to about 0.8. In the extreme

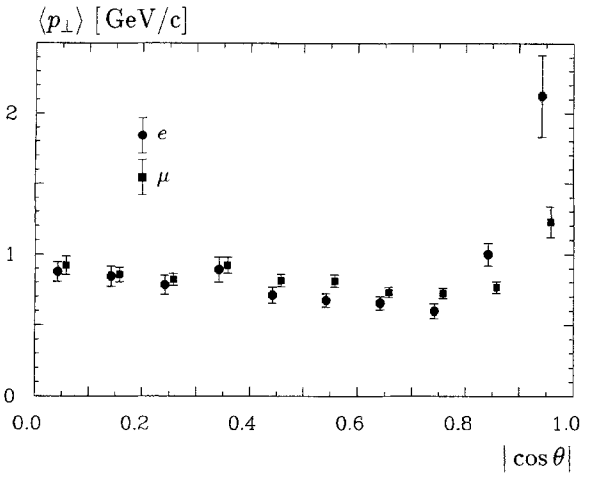

Fig. 2. $\langle p_\perp \rangle$ of e and μ candidates vs $|\cos\theta|$. $\langle p_\perp \rangle$ decreases by 20–30% up to $|\cos\theta| = 0.8$. The increase in the forward direction is caused by the large fluctuations of the $p_\perp$-measurement in a region, where many particles escape detection

forward direction particle losses affect the core of the jet and, together with a worse momentum resolution, lead to large fluctuations of the positively bounded variable $p_\perp$ and hence to an increase of $\langle p_\perp \rangle$. The effect is largest for electrons, which are only identified in the central part of the detector. These effects depend on the event topology and thus on the flavour of the event. For this reason $|\cos\theta|$ has to be included in the set of discriminating variables.

4 Probability densities

In the description of the event sample we distinguish six sources of leptons: prompt leptons (b or c), cascade leptons (bc) from the process $b \to c \to l$ and leptons from other sources or misidentified hadrons (bX, cX and uX). In the latter case we distinguish the background according to the primary flavour of the event*. Leptons from events with multiple leptons are treated as independent events and considered according to their respective **m**.

Each category i is characterized by a probability density $\rho_i(\mathbf{m})$, which is obtained from the Monte Carlo calculation. The likelihood $\mathscr{L}_j$ of an event j is constructed from the relative proportion p_i of each category i multiplied with the probability density.

$$\begin{aligned}\mathscr{L}_j = {} & p_b \cdot \rho_b(\mathbf{m}) \cdot \rho(\cos\theta, (1-2c_b)A_b) \\ & + p_{bc} \cdot \rho_{bc}(\mathbf{m}) \cdot \rho(\cos\theta, -(1-2c_{bc})A_b) \\ & + p_c \cdot \rho_c(\mathbf{m}) \cdot \rho(\cos\theta, -(1-2c_c)A_c) \\ & + p_{bX} \cdot \rho_{bX}(\mathbf{m}) \\ & + p_{cX} \cdot \rho_{cX}(\mathbf{m}) \\ & + p_{uX} \cdot \rho_{uX}(\mathbf{m}),\end{aligned}$$

* We use uX as a shorthand for all lepton candidates from light primary flavours u, d and s

The proportions p_i, $i = \{b, bc, \ldots\}$ are given by

$$\begin{aligned}p_i &= N_i / N_{\text{hadron}} \\ &= \tfrac{18}{11} Q_f^2 \varepsilon_i \,\mathrm{Br}(f \to l)_i + \alpha b_i \end{aligned} \quad (2)$$

where ε_i is the efficiency of detecting the lepton, Q_f the charge of the quark and $\mathrm{Br}(f \to l)$ the average leptonic branching ratio. The latter comprises an average over an imperfectly known composition of charmed particles with vastly different leptonic branching ratios. The first term is the dominant contribution for $i = b, bc$ and c while the background term αb_i describes the contribution from misidentified hadrons and background leptons. An overall factor α is chosen to account for the ignorance of the details of the processes contributing to the background and to account for overall differences in lepton rates observed between data and Monte Carlo. The proportions b_i are taken from the Monte Carlo simulation.

The additional probability densities ρ are defined as

$$\rho(\cos\theta, A) = \tfrac{3}{8}(1 + \cos^2\theta) + A\cos\theta. \quad (3)$$

They alone account for the angular distribution (and the asymmetry thereof) as long as the acceptance is symmetric in $\cos\theta$. The angle θ is measured between the incoming electron (positron) and the outgoing $f(\bar{f})$, were the direction of the flavour f is approximated by the thrust axis. The flavour or anti-flavour is defined experimentally by assuming production of a "naturally" charged lepton from b decay in the same event hemisphere. The background processes are assumed to be symmetric in polar angle. The asymmetries A of the quarks have to be modified to account for the charge confusion c_i of Table 2 according to

$$A^{\text{meas}} = (1 - 2c_i)A$$

as is shown in (1).

The overall likelihood function $\mathscr{L}$, which is to be maximized, is

$$\mathscr{L} = \prod_{\text{leptons}} \mathscr{L}_j.$$

5 Checks using Monte Carlo simulation

The Monte Carlo simulation has been used to verify the above ansatz. Figure 3 displays the reconstructed asymmetry A_b obtained in a 1 parameter fit as a function of the b quark asymmetry used in the simulation of the events. Similarly, for a 2 parameter fit of A_b and A_c, the analysis procedure reproduces various input asymmetries of the simulation (Fig. 4).

As a further check we measure the lepton branching ratios $\mathrm{Br}(b \to l)$, $\mathrm{Br}(c \to l)$ and the background contribution α (2), setting A_b and A_c to their input values. $\mathrm{Br}(b \to l)$ is reproduced within the statistical accuracy of the analysis. $\mathrm{Br}(c \to l)$, however, shows too strong a correlation with the background to be measured with the same reliability. The only term separating charmed from light quarks is the cascade contribution, which is rather small

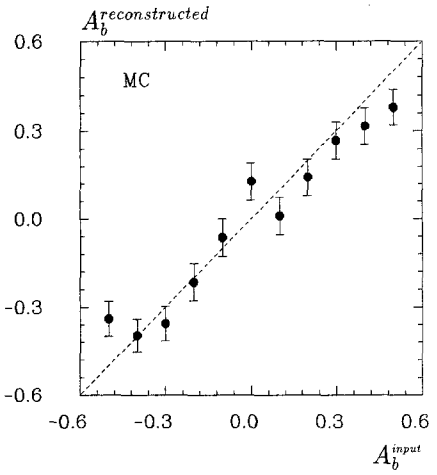

Fig. 3. Reconstructed asymmetry A_b versus Monte Carlo-input. A_c is fixed to -14% for this test

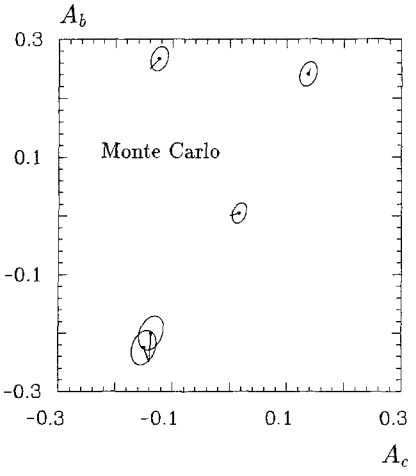

Fig. 4. Comparison of the reconstructed A_b and A_c from a 2 parameter fit with the input values used in the simulation. Solid lines are drawn between the input values of A_b and A_c and the reconstructed values. The ellipses indicate the $(\chi^2_{min}+1)$ contours

Table 3. A test of the fit procedure for the branching ratios of the Monte Carlo simulation. The fitted branching ratios Br_b (Br_c) are compared with the input branching ratios. A "1" indicates a fixed parameter and a number without errors a value resulting from the variation of the other parameters, constraining the total number of leptons to the observed value. The errors correspond to a change to $\chi^2_{min}+1$

Fit	$Br_b^{rec.}/Br_b^{input}$	$Br_c^{rec.}/Br_c^{input}$	α
Br_c free	1.14 ± 0.07	0.94	1
Br_c fixed	1.06 ± 0.06	1	0.98
2 Parameter	1.16 ± 0.06	0.66 ± 0.09	1.33

and itself overlapping with the prompt b contribution in the variable $m_\perp$. Table 3 lists the results of a typical analysis.

After these checks we are confident that both the ansatz (1) and the probability distributions obtained from the simulation are correct and behave as expected.

6 Results

In the analysis of the asymmetries of the real data the leptonic branching ratios are kept fixed. The branching ratios $Br(b\to e)$ and $Br(b\to\mu)$ are set to 11% in agreement with the values of [21]. For the charmed branching ratio we use the leptonic branching ratios of the individual charmed hadrons. This set of parameters results in a satisfactory description of the measured data for both types of leptons (Fig. 5).

6.1 2 Parameter fit

As a first step in the analysis, the beauty and charmed asymmetries are determined in a simultaneous fit to the experimental data. The results of the 2 parameter fits are summarized in Table 4 for all data periods and Fig. 6 displays the correlation between the fit parameters obtained at $\sqrt{s}=35$ GeV. The A_b and A_c measurements are correlated with a correlation coefficient ~0.3 in all cases except for the measurement using the 1982 μ data where the correlation coefficient is 0.68. The larger correlation is attributed to the higher background in the sample of μ-candidates during that period due to less efficient operation of the μ-chambers. An analysis using a tighter selection of μ-candidates with reduced background gives a coefficient of 0.38 for this sample.

Table 4. Results of the 2 parameter fit for A_b and A_c for the various data samples

$\sqrt{s}$	Sample	Period	A_b	A_c	Correlation
35	e	1982	$-4.5\pm14.9\%$	$-0.7\pm10.6\%$	0.28
35	μ	1982	$-17.6\pm9.2\%$	$-17.2\pm8.3\%$	0.68
35	e	1986	$-3.6\pm13.0\%$	$-6.6\pm7.5\%$	0.26
35	μ	1986	$-8.1\pm9.4\%$	$-11.6\pm7.1\%$	0.27
44	e	1985	$-13.3\pm26.1\%$	$-28.8\pm18.5\%$	0.32
44	μ	1985	$-14.9\pm19.4\%$	$11.5\pm15.9\%$	0.36

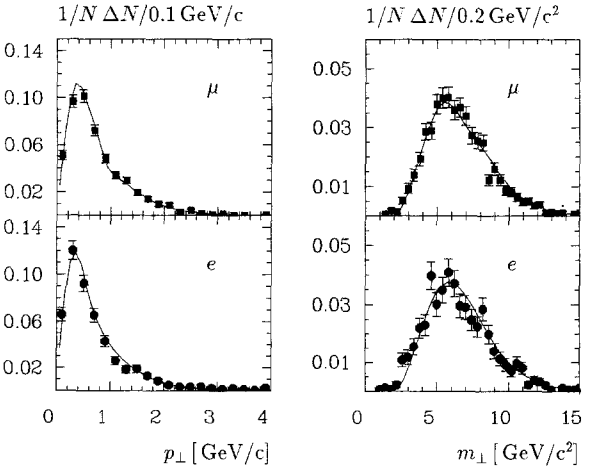

Fig. 5. $p_\perp$- and $m_\perp$-distributions for data of 1982 compared with the Monte Carlo (full line).

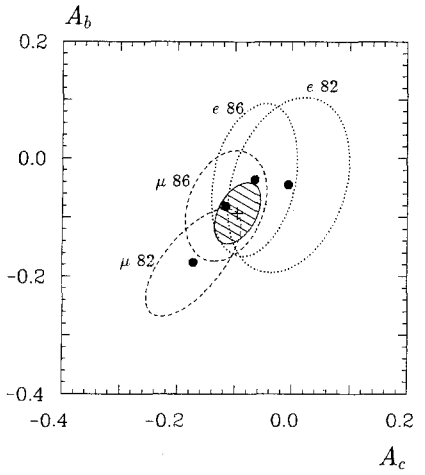

Fig. 6. $(\chi^2_{\min}+1)$-contour of the results of the 2 parameter fit A_c and A_b at 35 GeV. The shaded ellipse indicates the average of the measurements

The results for e and μ are statistically compatible and may be averaged to yield, at $\sqrt{s}=35$ GeV,

$$A_b = -9.3 \pm 5.2\%$$
$$A_c = -9.6 \pm 4.0\% \qquad (4)$$

with a correlation coefficient 0.44. The errors are statistical only.

Experimentally, this is the most general result of the analysis, since the least assumptions about the origin of the b and c asymmetries have been made. We continue the analysis in the framework of the Standard Model, which allows us to increase the precision in the individual measurement.

6.2 *The b asymmetry with constrained A_c*

Having obtained a nonzero asymmetry for both b and c quarks we constrain one asymmetry to the value of the Standard Model and extract the value of the other.

We start with a determination of A_b with the additional assumption that the asymmetry for c events is -14% (-23%) at $\sqrt{s}=35$ GeV (44 GeV), which corresponds to the theoretical values. The results for the various data samples are summarized in Table 5. The measurements for the e- and μ-samples are compatible with each other. We combine the results to get:

$$A_b = -11.6 \pm 4.8\% \quad \text{at 35 GeV and}$$
$$= -23.2 \pm 14.6\% \quad \text{at 44 GeV.} \qquad (5)$$

The result is based on 898 (154) leptons. A generous estimate of the statistical error is $1/\sqrt{N}=3.3\%$ (8.1%), which assumes a pure sample of signal events. This indicates that the statistical precision of this analysis is only moderately affected by the presence of background events in the sample.

Fitting in 5 separate $|\cos\theta|$-bins results in values for the asymmetries that can be converted into an acceptance corrected angular distribution, which is shown in Fig. 7. A_b (5) obtained from the overall Maximum Likelihood analysis describes well the angular dependence. The result of the A_b-measurements for μ and e in separate $|\cos\theta|$-bins is shown in Fig. 8. The sensitivity increases

Table 5. Results of the 1 parameter fit for A_b for the various data samples together with the number of leptons attributed to the direct decay

Data	$\sqrt{s}$	e		μ	
		A_b	$N_{b\to l}$	A_b	$N_{b\to l}$
1982	35	$-9.7\pm14.2\%$	161	$-15.3\pm7.1\%$	236
1986	35	$-7.0\pm12.5\%$	198	$-8.9\pm9.0\%$	303
Average combined	35	$-8.2\pm9.4\%$	359	$-12.8\pm5.6\%$	539
			$-11.6\pm4.8\%$		
1985	44	$-10.7\pm25.0\%$	58	$-29.6\pm17.9\%$	96
combined			$-23.2\pm14.6\%$		

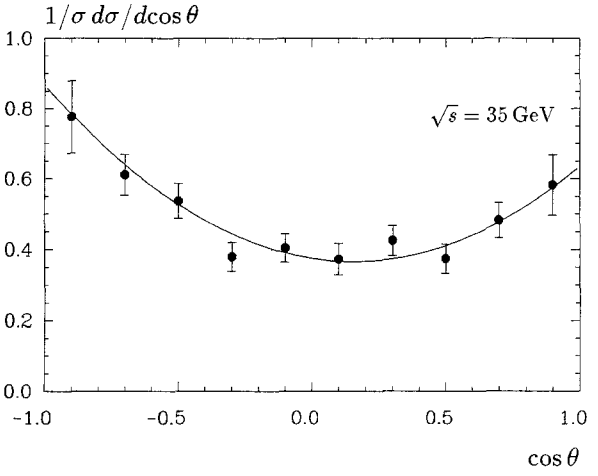

Fig. 7. Angular distribution of events $b\to l$ after acceptance correction together with the fit result $A_b=-11.6\pm4.8\%$. The errors shown are the poisson errors of the number of lepton events in the corresponding $\cos\theta$-bin

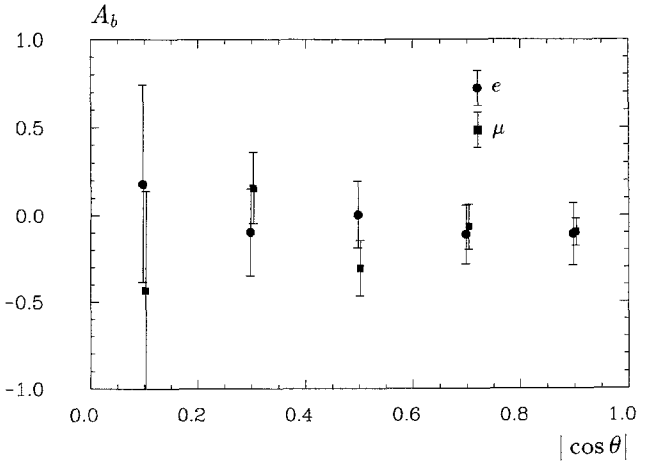

Fig. 8. A_b vs $|\cos\theta|$ for e- and μ-data. The two periods at 35 GeV have been averaged

with $|\cos\theta|$, as expected. Within the statistical uncertainty there is no dependence on $|\cos\theta|$, showing that the asymmetry is not the result of a particular angular part of the detector. The results for the e and μ samples are compatible.

6.3 *The c asymmetry with constrained A_b*

We are mainly interested in the value of the b asymmetry. For completeness we reverse the above procedure and extract the value of A_c alone. A determination of A_c when fixing A_b to the value of the Standard Model requires quantitative knowledge about $B\bar{B}$ mixing, notably of the effective mixing parameter χ.

If χ denotes the – time integrated – fraction of $\bar{B}$-hadrons that were originally produced as B, i.e.

$$\chi=\frac{N(B\to\bar{B})}{N(B)} \tag{6}$$

the resulting charge asymmetry is reduced to

$$A_b^{\text{mix}}=(1-2\chi)A_b. \tag{7}$$

The existing measurements of ARGUS and CLEO refer to oscillations in the $B_d\bar{B}_d$-system. In e^+e^--continuum production the measurements have to be extrapolated to oscillations of both neutral B-systems, i.e. B_d and B_s.

To assess the relative abundance of B_s^0 and B_d^0 we assume that the creation of "sea"-flavours is independent of the primary quark, so that we can apply the proportions

$$R_u:R_d:R_s=1:1:0.33 \tag{8}$$

for the frequencies of picking a light flavour from the vacuum to $b\bar{b}$-events. B_u^+ does not oscillate so that the effective mixing parameter χ can be written as

$$\chi=\frac{R_d\chi_d+R_s\chi_s}{R_u+R_d+R_s} \tag{9}$$

where we have assumed equal leptonic branching ratios for all B-hadrons. We have ignored possible contributions from b baryons. With [8] $\chi_d=0.17\pm0.05$ and complete mixing in the B_s^0-system ($\chi_s=0.5$), which is expected on theoretical grounds and also compatible with the measurement of UA1 [9] an effective mixing parameter $\chi=0.14$ for continuum production is obtained, which is applied in the analysis when constraining the value of A_b.

The results for the 1 parameter fits of A_c are shown in Table 6. The combined results for electron and muon samples are:

$$\begin{aligned} A_c &= -12.3\pm3.6\% \quad \text{at 35 GeV} \quad \text{and} \\ &= -9.1\pm11.3\% \quad \text{at 44 GeV.} \end{aligned} \tag{10}$$

Again, the errors are statistical only.

Table 6. Results of the 1 parameter fit for A_c for the various data samples together with the number of leptons attributed to the direct decay

Period	$\sqrt{s}$	e		μ	
		A_c	$N_{c\to l}$	A_c	$N_{c\to l}$
1982	35	$-3.2\pm10.1\%$	310	$-17.0\pm6.0\%$	572
1986	35	$-8.7\pm7.2\%$	381	$-13.5\pm6.8\%$	745
Average combined	35	$-6.8\pm5.9\%$	691	$-15.5\pm4.5\%$	1317
			$-12.3\pm3.6\%$		
1985	44	$-32.1\pm17.4\%$	113	$7.6\pm14.8\%$	215
combined			$-9.1\pm11.3\%$		

7 Systematic error

The separation of statistical and systematic errors is not unambiguous in a Maximum Likelihood analysis. Since there is no indicator of the quality of the fit an incorrect model (i.e. wrong probability distributions) may lead to an optimum with large errors, which reflect the *systematic* differences between the assumed probability distributions and the data. Some of the systematic effects considered in the following have been obtained by measuring the variation of the asymmetry as a function of the physical quantity under study and no attempt has been made to exclude such variations on the basis of the agreement with the data. The systematic uncertainties are summarized in Table 7. In detail, the following contributions have been investigated:

Table 7. Summary of the systematic errors. The total has been computed by adding the contributions in quadrature

Source	ΔA_b^{syst}			
	35 GeV		44 GeV	
	e	μ	e	μ
Selection	3.0%	4.0%	4.0%	6.0%
Charge confusion	2.0%	2.0%	2.0%	2.0%
Branching ratios	1.5%	1.5%	1.5%	1.5%
Charm asymmetry	1.5%	1.5%	2.0%	2.0%
Detector	1.5%	1.5%	1.5%	1.5%
Total ΔA_b^{syst} without "selection"	3.3%	3.3%	3.5%	3.5%
	ΔA_c^{syst}			
Selection	3.0%	4.0%	4.0%	6.0%
Charge Confusion	2.0%	2.0%	2.0%	2.0%
Branching ratios	1.5%	1.5%	1.5%	1.5%
$B\bar{B}$-Mixing	2.5%	2.5%	3.0%	3.0%
Detector	1.5%	1.5%	1.5%	1.5%
Total ΔA_c^{syst} without "selection"	3.8%	3.8%	4.2%	4.2%

Selection. This contribution comprises the dependence of the asymmetry measurement on the lepton selection procedure. The numbers given reflect the changes observed within different data samples when requiring tighter selection criteria for the lepton candidates. Such a procedure leads to a higher purity of the sample of μ-candidates and reduces the contribution of electrons from photon conversion in the e-sample. The variations observed are within statistical errors (maximum change $<3\sigma$). Alternatively, the changes can be interpreted as a measure of the lack of understanding of the detailed detector status as a function of time. We adopt the latter view and add this error to the statistical error of the result for each measurement.

Charge confusion. "Charge Confusion" enters in two places: Equation (1) explicitly requires knowledge of the contributions of the "wrong" sign leptons. The biggest contributions are observed in the cascade process, which constitutes $<10\%$ of the lepton sample. Model uncertainties in the factors of Table 2 are estimated $\Delta c_i<5\%$, so that the effect on the uncertainty of the asymmetry is $\sim 1\%$. The additional implicit assumption, however, is that the lepton candidates from background sources completely lose the memory of the primary flavour, i.e. $c_{bX}=c_{cX}=c_{uX}=0.5$. Derviations from this number lead to net asymmetries and are estimated from Monte Carlo simulations.

Branching ratios. The branching ratios assumed in the fit are varied within their respective experimental uncertainties [21]. The effect of the measurement of the asymmetries is small.

Table 8. The averages of the asymmetry measurements using a) statistical and b) statistical and systematic errors. Rows c) refer to the results of b) after inclusion of all corrections. The values of the Standard Model are also indicated

	$\langle A_b\rangle$*	
	$\sqrt{s}=35$ GeV	$\sqrt{s}=44$ GeV
a) Statistical average	$-11.6\pm4.8\%$	$-23.2\pm14.6\%$
b) Including systematic errors	$-11.4\pm5.3\pm3.3\%$	$-22.8\pm15.1\pm3.5\%$
c) Incl. corr., $\chi=0.14$ Standard model, lowest order	$-16.6\pm7.7\pm4.8\%$ -24.3%	$-33.6\pm22.2\pm5.2\%$ -39.9%

* A_c fixed

	$\langle A_c\rangle$*	
a) Statistical average	$-12.3\pm3.6\%$	$-9.1\pm11.3\%$
b) Including systematic errors	$-11.8\pm4.1\pm3.8\%$	$-10.0\pm11.9\pm4.2\%$
c) Including corrections Standard model, lowest order	$-12.8\pm4.4\pm4.1\%$ -13.6%	$-10.9\pm12.9\pm4.6\%$ -23.2%

* A_b fixed

Charm Asymmetry. The experimental value of the charm asymmetry is known with an accuracy $\Delta A_c\sim 3\%$. This leads to $\Delta A_b\leqq 2\%$ when fixing the value of A_c in the analysis.

$B\bar{B}$ Mixing. The experimental accuracy of the A_c-measurement has to be seen in conjunction with the knowledge of $B\bar{B}$ mixing. Within the experimental uncertainties we assume at most a 3% effect on A_c. For the A_b measurement itself mixing can be corrected for in the final result.

Detector. Asymmetries observed in event subsamples without lepton requirements lead to this upper limit on the systematic error. While such contributions may be expected within the Standard Model they affect the hypothesis of a completely symmetric background.

Inclusion of the "selection" uncertainty in the statistical error of (5) and (10) leads to the results of Table 8, row b). In all cases the final systematic error is the quadratic sum of the remaining systematic contributions as given in Table 7. The systematic errors for the two energies are strongly correlated.

8 Discussion

In the minimal version of the Standard Model the forward-backward charge asymmetry for $b\bar{b}$-production is – in lowest order – approximated by the product of the weak axial and electric charge of the produced quark times a factor which depends on the electroweak parameters. A recent analysis [22] of all electroweak data arrives at $\sin^2\theta_W=0.227\pm0.004$ without additional model assumptions. We use the m_Z measurement of [23] $m_Z=91.11\pm0.23$, which determines $\sin^2\theta_W=0.2312\pm0.0017$ by assuming for the top and Higgs mass $m_{\text{top}}=100$ GeV/c^2, $m_{\text{Higgs}}=100$ GeV/c^2. The resulting lowest order values of the asymmetry* are given in Table 8. Mass effects of the quarks have been included.

For comparison with these theoretical numbers several corrections have to be applied to the experimental data, which, in the following, are quoted as values δ_i such that $A=(1+\delta_i)A^{\text{exp}}$. Electroweak radiative corrections can be grouped into two types [25]. Corrections of the "QED"-type, i.e. with an extra photon added to the Born diagram, depend on the details of the experimental setup. The effect of initial state radiation, for example, reduces the observable asymmetry, for this experiment $\delta_{\text{em}}=6\%$, rather independent of the parameters of the Standard Model. In contrast, the "weak" corrections are in general noticeably affected by the choice of the electroweak parameters. However, at the energies dealt with in this analysis an uncertainty in the top mass $m_{\text{top}}=100\pm50$ GeV leads to an uncertainty in the prediction of the experimentally observed asymmetry

* In lowest order the parametrization of the theory is not unique. We apply the parameters of the neutral current sector, namely $\sin^2\theta_W$ and m_Z (cf. parametrization (II) of [24])

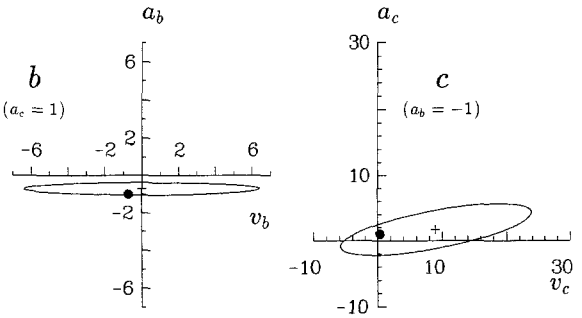

Fig. 9. The $(\chi^2_{\min}+1)$-error contour for the electroweak couplings of the b- and c-quark as a result of the asymmetry measurement. The dots indicate the values of the Standard Model

$\Delta A < 0.3\%$. For $m_{\text{top}} = 100\ \text{GeV/c}^2$ $\delta_{\text{weak}} \approx -1\%$ which is small in comparison with the present experimental accuracy.

QCD correction have been computed to first order only [26]. They amount to $\delta \approx 2.3\%$ for charmed and $\delta \approx -0.5\%$ for beauty quarks.

As mentioned before, the largest correction to the theoretical b asymmetry originates from $B\bar{B}$-mixing. We assume an effective mixing parameter $\chi = 0.14$, which is applied according to (7).

Applying all corrections to the measurements finally yields the corrected asymmetries of Table 8, rows c), in agreement with the predictions of the Standard Model. We combine both energies in a fit of the weak axial and vector charges a and v and obtain the error contours of Fig. 9. The experimental constraints on the vector charges are small despite the high energies available. A fit for the axial coupling alone results in

$$a_b = -0.72 \pm 0.34 \quad \text{with } a_c = 1 \quad \text{and}$$
$$a_c = \ \ 0.79 \pm 0.40 \quad \text{with } a_b = -1. \qquad (11)$$

The results are not independent since the other coupling is constrained to the value of the Standard Model as indicated. The errors include statistical and systematic contributions and correlations in the systematic errors have been taken into account.

Assuming validity of the minimal Standard Model we may express the experimental result as a measurement of $B\bar{B}$-mixing. This results in the value $\chi = 0.24 \pm 0.12$, which differs by two standard deviations from 0 and thus confirms the presence of mixing in the neutral B-system. If we assume complete mixing in the strange B-system we obtain a value $\chi_d = 0.40 \pm 0.28$.

9 Comparison with other measurements

An earlier result on A_b published by the JADE Collaboration [5] is based on a sample of events that has considerable overlap with the μ events used for this analysis. In fact, $\sim 80\%$ of the μ inclusive events for the data period of 1982 are contained in both analyses.

Changes in the event sample are due to substantial improvement in the track reconstruction (chamber calibration) with corresponding effects on the track selection. In addition, $\sim 10\%$ of the events included in the "1982" period of this analysis stem from data taken after finishing the earlier analysis. Therefore and for reasons of consistency we prefer to quote the results of this analysis as being valid for the entire JADE data sample.

If we restrict the new analysis to the overlap sample we obtain an asymmetry $A_b = -21\%$, which agrees well with the earlier result.

Measurements of the b quark asymmetry have been published by several other experiments*. A compilation of the results of the PETRA and PEP experiments is shown in Table 9 and Fig. 10. No correction for $B\bar{B}$ mixing has been applied, the errors quoted are statistical

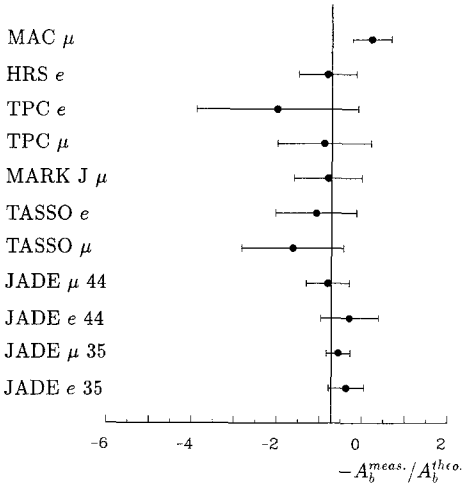

Fig. 10. Published values for $-A_b^{\text{meas}}/A_b^{\text{theo}} \approx (1-2\chi)\, a_b$ (assume $a_e = -1$). The experimental values have not been corrected for $B\bar{B}$ mixing. The solid line shows the lowest order expectation

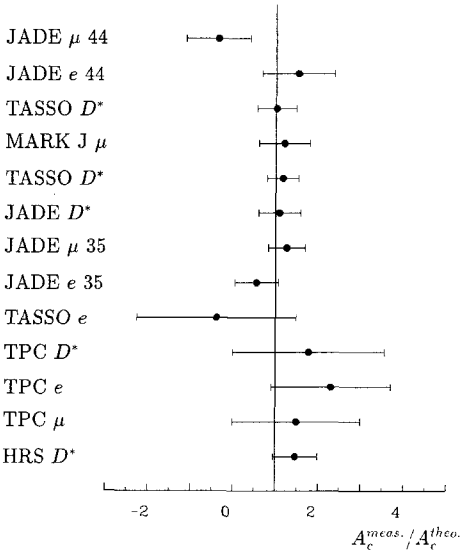

Fig. 11. Published values for $A_c^{\text{meas}}/A_c^{\text{theo}} \approx a_c$ (assume $a_e = -1$). The solid line shows the lowest order expectation

* After finishing this analysis we learned of a similar analysis of the CELLO Collaboration [27]

Table 9. Summary of the experimental results for the axial coupling of the b-quark

Experiment	Reference	$\sqrt{s}$ [GeV]	Method	A_b	$a_b^{\exp}$
JADE	this expt.	35.0	e	$-8.2\pm9.6\%$	-0.35 ± 0.41
JADE	this expt.	35.0	μ	$-12.7\pm6.3\%$	-0.55 ± 0.27
JADE	this expt.	44.0	e	$-10.7\pm25.3\%$	-0.28 ± 0.67
JADE	this expt.	44.0	μ	$-29.6\pm18.9\%$	-0.79 ± 0.50
TASSO	[28]	34.5	μ	$-37.5\pm27.5\%$	
TASSO	[29]	34.6	e	$-25.0\pm22.0\%$	
MARK J	[30]	35.3	μ	$-21.0\pm19.0\%$	-0.80 ± 0.80
TPC	[31]	29.0	μ	$-15.0\pm19.0\%$	-0.90 ± 1.10
TPC	[32]	29.0	e	$-34.0\pm32.0\%$	-2.00 ± 1.90
HRS	[6]	29.0	e	$-14.0\pm12.0\%$	-0.82 ± 0.68
MAC	[7]	29.0	μ	$3.4\pm7.0\%$	
Average					-0.51 ± 0.16
Average with $B\bar{B}$ mixing correction					-0.70 ± 0.22

Table 10. Summary of the experimental results for the charm asymmetry measurement. All errors are statistical

Experiment	Reference	$\sqrt{s}$ [GeV]	Method	A_b	$a_c^{\exp}$
HRS	[6]	29.0	D^*	$-14.0\pm5.0\%$	1.47 ± 0.52
TPC	[31]	29.0	μ	$-14.0\pm13.0\%$	1.50 ± 1.50
TPC	[32]	29.0	e	$-21.0\pm12.0\%$	2.30 ± 1.40
TPC	[33]	29.0	D^*	$-16.0\pm16.0\%$	1.78 ± 1.78
TASSO	[29]	34.6	e	$5.0\pm24.0\%$	
JADE	this expt.	35.0	e	$-6.8\pm6.3\%$	0.54 ± 0.50
JADE	this expt.	35.0	μ	$-15.4\pm5.3\%$	1.23 ± 0.42
JADE	[34]	35.0	D^*	$-14.9\pm6.7\%$	1.09 ± 0.49
TASSO	[35]	35.0	D^*	$-16.8\pm4.7\%$	1.16 ± 0.37
MARK J	[30]	35.3	μ	$-16.0\pm9.0\%$	1.20 ± 0.60
TASSO	[35]	36.2	D^*	$-16.0\pm7.2\%$	1.02 ± 0.46
JADE	this expt.	44.0	e	$-32.1\pm17.9\%$	1.50 ± 0.84
JADE	this expt.	44.0	μ	$7.6\pm16.0\%$	-0.36 ± 0.75
Average					1.07 ± 0.16

only and the value of the axial coupling has been computed from $-A_b^{\text{meas}}/A_b^{\text{theo}}$, the lowest order approximation. The computation of the average is based on the statistical errors only, since it is difficult to assess the correlation of systematic effects between different experiments. The average is dominated by the measurement of this experiment (11).

The list of experiments contributing to the measurement of a_c is longer (Table 10, Fig. 11). In addition to the lepton analysis the "D^*-method" provides a powerful tool in c-quark studies. The measurements, when expressed as energy independent weak couplings, are well compatible with each other and with the value of the Standard Model.

Acknowledgements. We are indebted to the PETRA machine group and the DESY computer centre staff for their excellent support during the experiment and to all the engineers and technicians of the collaborating institutions who have participated in the construction and maintenance of the apparatus. This experiment was supported by the Bundesministerium für Forschung und Technologie, by the Ministry of Education, Science and Culture of Japan, by the UK Science and Engineering Research Council through the Rutherford Appleton Laboratory and by the US Department of Energy. The visiting groups at DESY wish to thank the DESY directorate for the hospitality extended to them.

References

1. W. Ash et al. MAC Coll.: Phys. Rev. Lett. 58 (1987) 1080
2. T. Greenshaw et al. JADE Coll.: Z. Phys. – Particles and Fields C 42 (1989) 1
3. F. Ould-Saada: DESY 88–177 (1988)
4. R. Marshall: Z. Phys. – Particles and Fields C 26 (1984) 291
4. W. Bartel et al. JADE Coll.: Phys. Lett. 146 B (1984) 437
6. C.R. Ng et al. HRS Coll.: ANL-HEP-PR-88-11 (1988)
7. H.R. Band et al. MAC Coll.: Phys. Lett. 218 B (1989) 369
8. H. Albrecht et al. ARGUS Coll.: Phys. Lett. 192 B (1987) 245
9. C. Albajar et al. UA1 Coll.: Phys. Lett. 186 B (1987) 247; err. ibid. 197 B (1987) 565
10. W. Bartel et al. JADE Coll.: Phys. Lett. 88 B (1979) 171; B. Naroska: Phys. Rep. 148 B (1987) 67
11. J. Allison et al.: Nucl. Instrum. Methods A 238 (1985) 220–229
12. W. Bartel et al. JADE Coll.: Phys. Lett. 129 B (1983) 145
13. G. Eckerlin et al.: IEEE Trans. Nucl. Sci. NS-34 (1987) 182

14. K.-H. Hellenbrand: PhD thesis, University of Heidlberg, (1987)
15. J. Allison et al.: Nucl. Instrum. Methods A 238 (1985) 230–237
16. W. Bartel et al. JADE Coll.: Z. Phys. C 33 (1987) 339
17. J. Chrin: Z. Phys. C 36 (1987) 163
18. M. Zimmer: PhD thesis, University of Heidelberg (1989)
19. T. Sjöstrand: Comput. Phys. Commun. 43 (1987) 367
20. T. Sjöstrand: LU-TP-85-10 (1985)
21. G.P. Yost et al.: Phys. Lett. 204 B (1988) 1
22. D. Haidt: Proceedings of the Europhysics Conference on High-Energy Physics, Madrid 1989, to be publ. in Nucl. Phys. B
23. G.S. Abrams et al. MARK II Coll.: Phys. Rev. Lett. 63 (1989) 724
24. W. Bartel et al. JADE Coll.: Z. Phys. C 26 (1985) 507
25. W.F.L. Hollik: DESY 88-188 (1988)
26. J. Jersak et al.: Phys. Lett. 98 B (1981) 363
27. H.J. Behrend et al. CELLO Coll.: DESY 89/125 (1989)
28. M. Althoff et al. TASSO Coll.: Z. Phys. C 22 (1984) 219
29. M. Althoff et al. TASSO Coll.: Phys. Lett. 146 B (1984) 443
30. B. Adeva et al. MARK J Coll.: Phys. Rept. 109 (1989) 131
31. H. Aihara et al. TPC Coll.: Phys. Rev. D 31 (1985) 2719
32. H. Aihara et al. TPC Coll.: Z. Phys. C 27 (1985) 39
33. H. Aihara et al. TPC Coll.: Phys. Rev. D 34 (1986) 1945
34. F. Ould-Saada et al. JADE Coll.: DESY 89/063 (1989)
35. W. Braunschweig et al. TASSO Coll.: DESY 89/053 (1989)